Construction and Building Materials 26 (2012) 638–654

Contents lists available at ScienceDirect

Construction and Building Materials

journal homepage: www.elsevier.com/locate/conbuildmat

Mechanical properties of foamed concrete exposed to high temperatures

Md Azree Othuman Mydin [a,*], Y.C. Wang [b]

[a] School of Housing, Building and Planning, Universiti Sains Malaysia, 11800 Penang, Malaysia
[b] School of Mechanical, Aerospace and Civil Engineering, University of Manchester, Manchester M60 1QD, UK

ARTICLE INFO

Article history:
Received 12 November 2010
Received in revised form 5 June 2011
Accepted 18 June 2011
Available online 23 July 2011

Keywords:
Foamed concrete
Mechanical properties
High temperatures
Elevated temperatures
Concrete model
Strength prediction model
Stress–strain
Concrete in fire

ABSTRACT

This paper reports the results of an experimental and analytical study to investigate the mechanical properties of unstressed foamed concrete exposed to high temperatures. Two densities of foamed concrete, 650 and 1000 kg/m^3, were made and tested with additional tests being performed on densities of 800, 1200 and 1400 kg/m^3 for additional data. The experimental results consistently demonstrated that the loss in stiffness for foamed concrete at elevated temperatures occurs predominantly after about 90 °C, regardless of density as water expands and evaporates from the porous body. From a comparison of the experimental results of this research with a number of predictive models for normal strength concrete, this research has found that the mechanical properties of foamed concrete can be predicted using the mechanical property models for normal weight concrete given that the mechanical properties of foamed concrete come from Portland Cement CEM1.

1. Introduction

Foam concrete is a lightweight material consisting of Portland cement paste or cement filler matrix (mortar) with a uniformly distributed pore structure produced by mechanically introducing air in the form of small bubbles having a total volume of at least 20%. Foamed concrete can be designed to have any density in the range of 400–1600 kg/m^3. It has a number of attractive characteristics such as good thermal and acoustic insulation, self-flowing and easy to produce. Although foamed concrete has low mechanical properties compared to normal strength concrete, it may be used as partition or load bearing wall in low-rise residential construction. Before it can be considered for use as a load bearing material in the building industry, it is necessary to acquire reliable information on mechanical properties of foamed concrete at ambient and elevated temperatures for quantification of its fire resistance performance.

Foamed concrete may be considered a three phase material with cement paste, aggregate (fine sand) and air voids. Consequently, the degradation mechanisms of foamed concrete are mainly caused by deprivation of the cement paste. When exposed to high temperatures, the chemical composition and physical structure of foamed concrete change significantly due to changes in the cement paste.

The degradation mechanisms of foamed concrete upon exposure to elevated temperatures include chemical degradation and mechanical deterioration where each mechanism is dominant within a specific temperature range. Chemical degradation occurs when the chemically bound water is released from the cement paste. The dehydration process in the cement paste becomes significant at temperatures above about 110 °C [1] and diminishes the calcium silicate hydrate (CSH) links which provide the primary load-bearing formation in the hydrated cement. Furthermore, due to low permeability of the cement paste, internal water pressure is built up during dehydration of the hydrated CSH, which increases internal stresses and induce microcracks in the material from about 300 °C, resulting in decreased strength and stiffness of foamed concrete [2,3]. At higher temperatures around 530 °C, calcium hydroxide ($Ca(OH)_2$) dissociates, resulting in the shrinkage of foamed concrete. If the hot foamed concrete is exposed to water, as in fire fighting, CaO in foamed concrete turns into $Ca(OH)_2$ to cause cracking and destruction of foamed concrete. However, it is still extremely difficult to accurately predict these mechanisms and experimental investigation remains essential.

Thus, the main objective of this work is to provide experimental data on the mechanical properties of foamed concrete at elevated temperatures. Therefore only a constant cement–sand ratio of 2:1 and water–cement ratio of 0.5 will be used for all batches of foamed concrete samples made for this research. Tests were carried out at temperatures at about 20 (ambient temperature), 100, 200, 300, 400, 500, and 600 °C for ease of observation of the test results. Extensive compressive and bending strength tests were

* Corresponding author. Tel.: +60 4 6532813.
E-mail address: md_azree@hotmail.com (M.A.O. Mydin).

0950-0618/$ - see front matter © 2011 Elsevier Ltd. All rights reserved.
doi:10.1016/j.conbuildmat.2011.06.067

carried out for foamed concrete of densities of 650 kg/m^3 and 1000 kg/m^3. Based on these experimental results, prediction equations will be proposed, based on comparison of the experimental results with existing models for normal weight concrete. It should be pointed out that this research is not trying to solve the problem of how changing the percentage of each of the three phases (cement, sand and void) would change the foamed concrete property but the authors are trying to find a method to quantify foamed concrete mechanical properties at elevated temperatures given that the properties at ambient temperature are known.

2. Experimental setup

The foamed concrete used in this study was made from ordinary Portland Cement CEM1, fine sand, water and stable foam and Table 1 lists details of the constituent materials. The cement–sand ratio was 2:1 and the water–cement ratio was maintained at 0.5. A higher cement–sand ratio (2:1) was chosen to achieve better compressive strength and water–cement ratio of 0.5 was found acceptable to achieve adequate workability [6]. Two densities of foamed concrete, 650 and 1000 kg/m^3, were cast and tested. The 650 kg/m^3 density was selected as it may be used in lightweight partition and the 1000 kg/m^3 density was considered because foamed concrete of this density would have a useful amount of mechanical properties to make it practicable as a light load bearing infill material, which may be combined with profiled thin walled steel in lightweight composite panel construction. Further details of the mix constituent proportions of both densities are outlined in Table 2. The target foam concrete volume required for each mix design was 0.1 m^3.

2.1. Specimen preparation

All the foamed concrete samples were made in house. The stable foam was produced using foam generator Portafoam TM2 System, obtained from the Malaysian manufacturer (www.portafoam.com). This system runs from an air compressor and consists of a main generating unit, a foaming unit, and a lance unit. The foaming agent used was Noraite PA-1 (protein based) which is appropriate for foamed concrete densities ranging from 600 kg/m^3 to 1600 kg/m^3. Noraite PA-1 comes from natural sources and has a weight of around 80 g/l and expands about 12.5 times when used with the Portafoam foam generator. Three identical specimens were prepared for each density and were tested at 28 days after mixing.

2.2. Heating of specimens

Two different electric furnaces were used for heating the foamed concrete specimens to the various steady-state temperatures. One furnace had a maximum operating temperature of 450 °C (low temperature furnace), and the second furnace had a maximum operating temperature of 1000 °C (high temperature furnace). Each of the furnaces was capable of holding three specimens. The low temperature furnace had a temperature range of 50–450 °C and was used for four of the reported thermal exposure conditions: 100 °C, 200 °C, 300 °C and 400 °C. The furnace temperature exposure profiles were produced by a programmable microprocessor temperature controller attached to the furnace power supply and monitored by a Type K thermocouple located in the furnace chamber. The high temperature furnace (Fig. 1) had a maximum operating temperature of 1000 °C. This furnace was used for exposing concrete specimens to 500 °C and 600 °C. This furnace was also controlled by a programmable microprocessor temperature controller attached to the furnace power supply based on feed-back temperature reading from a Type K thermocouple located in the furnace chamber. Pre-testing checking of the furnaces showed that both furnace controllers and furnace power system could maintain furnace operating temperatures within ±1 °C over the test range.

2.3. Test overview

A variety of test methods may be used to obtain different aspects of mechanical properties of materials at high temperatures, including the stressed test, the unstressed test, and the unstressed residual strength test [7]. In this research, the unstressed test method was adopted for convenience. In the unstressed test, the

Fig. 1. High temperature electric furnace with specimens.

Table 1
Constituent materials used to produce foamed concrete.

Constituents	Type
Cement	Portland Cement CEM1 [4]
Sand	Fine sand with additional sieving to eradicate particles greater than 2.36 mm, to improve the foamed concrete flow characteristics and stability [5]
Stable foam	Noraite PA-1 (protein based) surfactant with weight of around 70–80 g/l produce from Portafoam TM2 System. The surfactant solution consists of one part of surfactant to 33 parts of water.

Table 2
Mix constituent proportions of foam concrete mixes.

Target dry density (kg/m^3)	Target wet density (kg/m^3)	Cement:sand	Water:cement	Portland cement content (kg/m^3)	Sand content (kg/m^3)	Noraite PA-1 surfactant (m^3)
650	774	2:1	0.5	39	19	0.063
1000	1136	2:1	0.5	57	28	0.045

sample was heated, without preload, at a steady rate to the predetermined temperature. While maintaining the target temperature, load was applied at a prescribed rate until sample failure. Because the temperature is unchanged, the test is also referred to as steady state test, as opposed to transient test in which the specimen temperature changes with time.

2.4. Compression test setup

The compressive strength tests were carried out on 100 × 200 mm cylinders. The specimens were removed from moulds after 24 h of casting and then seal cured in domestic cling film for 28 days. Prior to testing, the specimens were removed from the curing tank and put in the oven for 24 h at 105 °C. After 24 h, all the specimens were removed from the oven and their ends were ground flat. To monitor the strain behavior at ambient temperature during loading, two strain gauges was fitted on each sample for the ambient test only. Since no strain measurement was made at elevated temperatures, the ambient temperature strain measurements were used to confirm that the strain calculated based on the displacement of the loading platen was of sufficient accuracy. Four Type K thermocouples were installed in the central plane of each cylinder specimen as shown in Fig. 2.

Loading was applied using an ambient temperature machine after removing the test samples from the furnace. To minimise heat loss from the specimen to atmosphere, each specimen was wrapped with insulation sheets immediately after being removed from the electric furnace. For each set of test, three replicate tests were carried out to check consistency of results. The target temperatures were 20 °C (room temperature), 100, 200, 300, 400, 500, and 600 °C. During the loading process, the temperature of each sample (thermocouple T3) was measured and it was found that the temperature was stable throughout the testing period. Fig. 3 shows typical temperature variations throughout the loading phase for specimens of 1000 kg/m^3 density. As can be seen, because the duration of loading was short (just over one minute), there was very little heat loss and the temperature change was less than 0.5 °C.

2.5. Three point bending test setup

Three methods may be used to obtain the tensile strength of concrete: direct tensile test, tensile splitting test or flexural (three point bending) test. For convenience in this study, the three point bending test was carried out. The preparation of samples followed

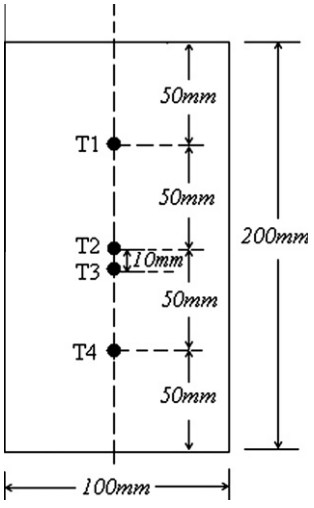

Fig. 2. Typical 100 × 200 mm cylinder specimen with thermocouples arrangement.

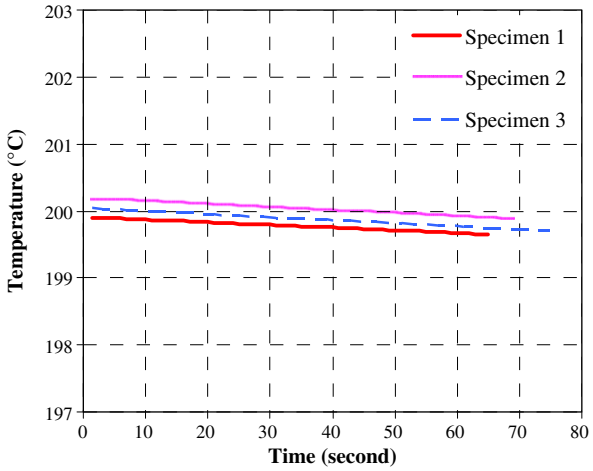

Fig. 3. Temperature change during test of specimens of 1000 kg/m^3 density at target temperature of 200 °C.

a similar procedure as outlined above for the compression tests. The specimens were rectangular parallelepipeds of height (h) 25 mm, width (w) 125 mm and length L (l) 350 mm. The specimen was simply supported and was subjected to point load at the centre point. The length between the supports was L_s = 200 mm, giving a L_s/h aspect ratio of 8 and sufficient to ensure predominance of bending behavior. The load–deflection was recorded for the evaluation of flexural tensile strength. Assuming linear elastic behavior, the maximum flexural bending strength (f_{cr}) is at the centre (point B) which is defined as:

$$f_{cr} = \left(\frac{1}{4}PL\right) \Big/ \left(\frac{bd^2}{6}\right) = \frac{3PL}{2bd^2} \tag{1}$$

where $\frac{1}{4}PL$ is the bending moment at point B and $\frac{bd^2}{6}$ is the elastic modulus for rectangular cross-section. The flexural strength becomes tensile strength only if the material behavior is linear until tensile failure.

The flexural modulus of elasticity may be calculated using the following equation:

$$E_{cr} = \frac{PL^3}{4bd^3y} \tag{2}$$

where y is the maximum deformation at the centre of the beam.

2.6. Porosity measurements

Porosity in foamed concrete plays a major role in determining its mechanical properties. Determination of porosity is, in fact, a quite complex problem. In this study, the porosity of foamed concrete was determined through the Vacuum Saturation method [8]. The measurements of foamed concrete porosity were conducted on slices of 68 mm diameter cores cut out from the centre of 100 mm cubes. The specimens were heated to predetermined temperature (ambient, 200 °C, 400 °C and 600 °C) until constant weight had been attained and were then placed in a desiccator under vacuum for at least 3 h, after which the desiccator was filled with de-aired, distilled water. The porosity was calculated using the following equation:

$$P = \frac{(W_{sat} - W_{dry})}{(W_{sat} - W_{wat})} \times 100 \tag{3}$$

where P = porosity (%); W_{sat} = weight in air of saturated sample; W_{wat} = weight in water of saturated sample and W_{dry} = weight of oven-dried sample. The measured results are given in Table 3.

Table 3
Porosity of foamed concrete obtained through vacuum saturation apparatus.

Density (kg/m^3)	Sample	Porosity (%)			
		Ambient	200 °C	400 °C	600 °C
650	1/1	74.8	74.9	75.9	76.3
	1/2	74.7	74.9	75.7	76.1
	1/3	74.8	75.0	76.1	76.5
1000	1/4	49.7	49.9	52.4	53.4
	1/5	50.0	50.4	52.5	53.7
	1/6	50.4	50.7	52.9	54.1

Table 3 indicates that the different replicate samples of the same test give consistent results.

3. Results and discussion

3.1. Effects of high temperature on foamed concrete density

Hydrated cement paste is composed from four major compounds of tricalcium silicate ($3CaO{\cdot}SiO_2$), dicalcium silicate ($2CaO{\cdot}SiO_2$), tricalcium aluminate ($3CaO{\cdot}A1_20_3$) and tetracalcium aluminoferrite ($4CaO{\cdot}A1_20_3{\cdot}Fe_20_3$). The most significant products involved in hydration reactions are calcium silicate hydrate (C-S-H) and portlandite, also called calcium hydroxide ($Ca(OH)_2$).

Foamed concrete contains free water and chemically bond water. The free water content in foamed concrete depends on the density (i.e., the free water content for the 650 kg/m^3 density is 1% by weight and for the 1000 kg/m^3 density is 2% by weight based on experiment data). Evaporation of the free and some of the chemically bond water will cause dehydration in foamed concrete, which will affect all the three items of thermal properties of foamed concrete (density, specific heat and thermal conductivity).

The dehydration process starts as early as 90 °C. In the range of 90–170 °C, the evaporable free water and part of the chemically bond water escapes. The evaporable free water may be considered to have been completely eliminated by 170 °C. Some chemically bond water is also lost through decomposition of the calcium silicate hydrates (C-S-H) gel that takes place between 120 °C and 140 °C and decomposition of ettringite around 120 °C [9]. In the temperature range between 200 °C and 300 °C, some of the chemically bond water is released from further decomposition of the C-S-H gel and the sulfoaluminate phases ($3CaO{\cdot}Al_2O_3{\cdot}CaSO_4{\cdot}12H_2O$ and $3CaO{\cdot}Al_2O_3{\cdot}3CaSO_4{\cdot}31H$) of the cement paste [9]. Further dehydration occurs at around 450 °C, which corresponds to decomposition of $Ca(OH)_2 \rightarrow CaO + H_2O$ [9] and it is completed at 530 °C. At the second dehydration reaction, 75% of the chemically combined water is vaporised and the remaining 25% is then evaporated at the third dehydration reaction.

The previously described three stages of dehydration are accompanied by water loss or reduction in density of foamed concrete. Fig. 4 shows recorded densities of foamed concrete at different temperatures, as ratio of the original density for two different initial density values, 650 kg/m^3 and 1000 kg/m^3. These values are also compared to the density change of mortar (density 1850 kg/m^3).

The results presented in Fig. 4 were obtained by directly weighing samples after heating them to different temperatures. Usually thermo gravimetric analysis (TGA) may be performed to determine changes in weight at increasing temperatures. However, due to limitation in experimental facility, this study used manual recording according to the following procedure: three 100 × 100 mm × 100 mm foamed concrete cubes of each density (650, 1000 and 1850 kg/m^3) were heated to different temperatures and then kept at the desired temperature for 24 h. Their weight was recorded afterwards to obtain weight loss. The procedure was kept on until a maximum temperature of 1000 °C.

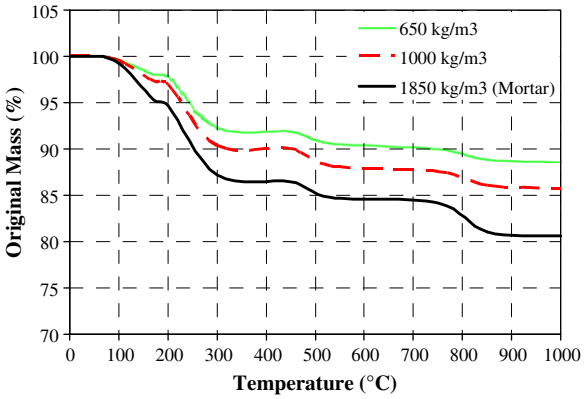

Fig. 4. Percentage of original density at different temperatures.

The three curves are similar and the three dehydration phases can be clearly seen in Fig. 4. This figure also shows a further weight loss phase, occurring between 750 °C and 850 °C, which can be assigned to the release of carbon dioxide (CO_2) from calcium carbonate ($CaCO_3$) [9]:

$$CaCO_3 \rightarrow CaO + CO_2$$

Table 4 summarises the density change values for the four phases (three phases of dehydration and final phase of CO_2 release) of weight loss.

3.2. Effect of high temperature on porosity of foamed concrete

The pore structure of cementitious material, predetermined by its porosity, is a very significant characteristic as it influences the properties of the material such as strength and durability. The porosity could therefore be a major factor influencing the material properties of foamed concrete and an in depth look into this aspect is essential to determine the relationships between porosity and material properties. Generally, the mechanical properties of foamed concrete decrease with increasing porosity. The density of foamed concrete may be diverse for the same water–cement ratio, through the integration of different amounts of foam, which may result in a different porosity and void sizes. For that reason, any change in the micro structure of foamed concrete due to a variation in the void system may influence the mechanical properties considerably in relation to density.

Usually, the porosity of cement based material changes when the temperature increases. These changes in porosity can be characterized by considering phase changes in the concrete at different temperatures. Kalifa et al. [10] in their research credited the increase in porosity with temperature to the release of chemically bound water and to the microcracking produced by expansion of the cement paste. Gallé and Sercombe [11] attributed the growth of porosity to the formation of large capillary pores in the concrete which corresponds to the release of adsorbed water in capillary pores and release of chemically bound water in the hydrated cement paste. Gallé and Sercombe [11] observed that macropores correlated to microcracks observed at the surface of specimens heated beyond 250 °C. During the heating process, the authors observed from 300 °C a number of cracks on the foamed concrete specimens due to the heating, which could be concurrent to the growth of porosity and microstructure changes. Ye et al. [12] attributed the increase in porosity due to the decomposition of calcium silicate hydrate (CSH) and calcium hydroxide (CH). These transformations formed additional void spaces in heated concrete.

Table 4
Density change values due to the dehydration and gas release process.

Actual density (kg/m^3)	Remaining density at the end of each phase (kg/m^3)				
	Oven dried density	(1th) Completed at 170 °C	(2nd) Completed at 300 °C	(3rd) Completed at 530 °C	(Final) completed at 850 °C
650	642	637	603	590	579
1000	983	973	903	881	860
1850	1803	1763	1613	1569	1500

Fig. 5 presents the total porosity for each mix as a function of the temperature. Foamed concrete of both densities experienced a slight monotonous increase in porosity with temperature. The initial porosity for 650 and 1000 kg/m^3 density was 74.8% and 50.0% respectively. Between 200 °C and 300 °C, the porosity increased considerably for the higher density foamed concrete while the increase was more moderate for the lower density foamed concrete due to decomposition of the different amounts of calcium silicate hydrate gel and sulfoaluminate. At 300 °C, the measured porosity for 650 and 1000 kg/m^3 density was 75.5% and 51.9% correspondingly. For temperatures beyond 400 °C, the measured porosity showed some increase corresponding to the decomposition of calcium hydroxide to form calcium oxide. At 600 °C, the porosity was 76.3% and 53.7% for 650 and 1000 kg/m^3 respectively. Nevertheless, in general, due to the high porosity at ambient temperature, foamed concrete may be considered to have constant porosity at different temperatures.

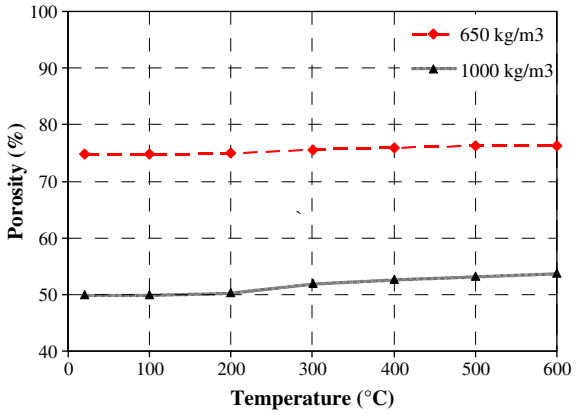

Fig. 5. Porosity of foamed concrete of two initial densities as a function of temperature.

3.3. Effects of high temperature on compressive strength of foamed concrete

As will be shown later in Section 3.4, the three duplicate tests of each series gave very consistent results so the average results may be used. As expected, for both densities, the foamed concrete compressive strength decreased with temperature. Fig. 6 presents the compressive strength and normalized compressive strength of foamed concrete at different temperatures. On initial heating, the foamed concrete made with Portland Cement CEM1 lost the absorbed, evaporable (or free) water and then the chemically bound water. The loss of water would induce micro cracking resulting in a reduction in strength. Between 90 °C to 170 °C, the compressive strength decreased slowly due to the release of free water and some of the chemically bound water. According to Khoury [13], the decrease in compressive strength between 20 and 150 °C corresponds to a reduction of the cohesion of the Van der Waal forces between the calcium silicate hydrate layers. This decreases the surface energy of calcium silicate hydrate and leads to the formation of silanol groups (Si–OH: OH–Si) that presents weaker bonding strength. However, because this change only affects the concrete superficially, the reduction in concrete strength is not significant and the compressive strength of the foamed concrete samples at 200 °C still retained about 94% of the original unheated value. Between 200 °C and 400 °C, decomposition of C-S-H gel and the sulfoaluminate phases caused cracks in the specimens [9]. These cracks had significant effects on the compressive strength of foamed concrete [3]. At 400 °C, the foamed concrete strength retained only about 75% of its initial value for both densities. Further degradation and loss of strength continued to take place at high temperatures. At temperature of 600 °C, the foamed concrete retained only about 40% of the original strength for both densities.

Since the compositions of both densities of foamed concrete are identical, except for increased pores in the lower density foamed concrete, it is not surprising that the normalized strength – temperature relationships of foamed concrete of both densities are almost the same.

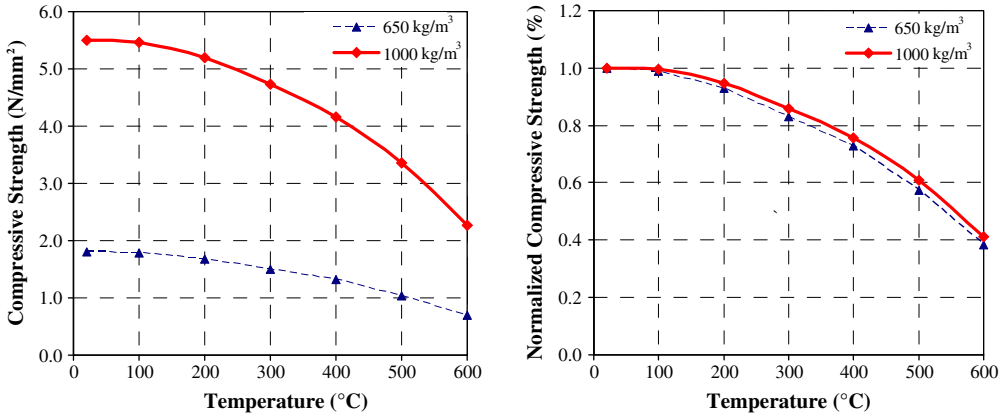

Fig. 6. Compressive strength (left) and normalized compressive strength (right) of foamed concrete as a function of temperature.

3.4. Effects of high temperature on compressive stress–strain relationship of foamed concrete

The engineering stress–strain relationships of foamed concrete were determined from the measured load and deflection results using the original specimen cross-sectional area A_o and length L_o. Due to difficulty of using strain gauges at high temperatures, the deflection used to calculate the strain was that of the movement of the loading platen. To confirm this method, strains were measured at ambient temperature. Fig. 7 compares the measured strain and that calculated using the displacement of the loading platen for the ambient temperature test. This comparison demonstrates that it is sufficiently accurate to use the loading platen displacement to calculate the axial strain of the test specimen.

The tests were displacement controlled where the crack continue to develop and grow after the peak load is reached. Since the test specimens failed in a brittle manner after reaching the peak stress, it was not possible to obtain the descending branch of the stress–strain relationship. Fig. 8 presents the average stress–strain curves at all different testing temperatures for the two densities.

For both densities at all temperature levels, the ascending branch was linear for stress up to 75% of the peak strength. The strain corresponding to the peak strength increased at increasing temperatures. For foamed concrete of 650 kg/m^3 density, the maximum strains were 0.0034, 0.0039, 0.0055 and 0.0066 at ambient temperature, 200 °C, 400 °C and 600 °C respectively; for the 1000 kg/m^3 density, the corresponding values were 0.0024, 0.0029, 0.0039 and 0.0048 at ambient, 200 °C, 400 °C and 600 °C respectively. The increase in strain results from opening of cracks initiated by the heating at higher temperatures.

Table 5 shows, for both densities and all temperatures, the elastic strain at the maximum stress, the maximum strain at the maximum stress and the ratio of these two strains. It appears that an average constant ratio of about 1.78 may be used for all cases.

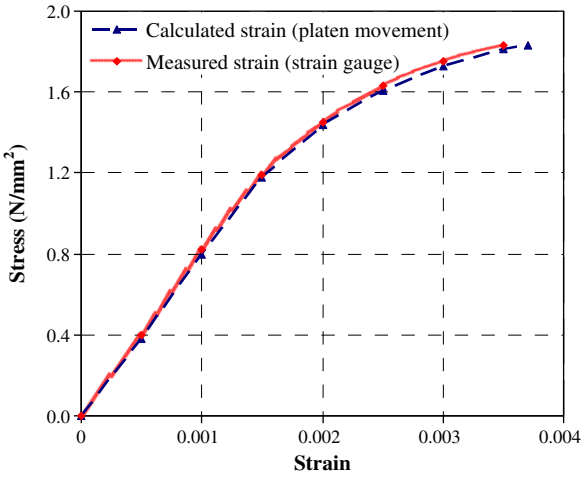

Fig. 7. Comparison of measured strain and calculated strain (based on movement of the loading platen) for foamed concrete of 650 kg/m^3 density at ambient temperature.

3.5. Effect of high temperature on modulus of elasticity of foamed concrete in compression

Fig. 9 demonstrates the changes in modulus of elasticity of foamed concrete in compression as a function of temperature. The modulus of elasticity was taken as the secant modulus at the point where the material changed from elastic to plastic behavior from the experimental compressive stress–strain curve. Compared to the reduction in foamed concrete strength, the reduction in elastic modulus is greater. Both figures show that the loss in modulus of elasticity began immediately upon heating when the samples began to dry. The modulus of elasticity at 200 °C, 400 °C and 600 °C was respectively about 75%, 40% and 25% of the original value for both densities. As with changes in normalized strengths of foamed concrete of both densities at elevated temperatures, the normalized modulus of elasticity of foamed concrete of both densities at the same temperature was almost the same.

Table 5
Elastic microstrain at the maximum stress, maximum microstrain at the maximum stress and the ratio of these two strains for both densities at different temperatures.

Density (kg/m^3)	Temperature (°C)	Elastic microstrain at maximum stress	Maximum microstrain at maximum stress	Ratio of maximum microstrain at peak stress to elastic microstrain at peak stress
650	Ambient	1900	3400	1.79
	200	2200	3900	1.77
	400	3000	5500	1.83
	600	3700	6600	1.78
1000	Ambient	1300	2400	1.85
	200	1600	2900	1.81
	400	2300	3900	1.70
	600	2800	4800	1.71

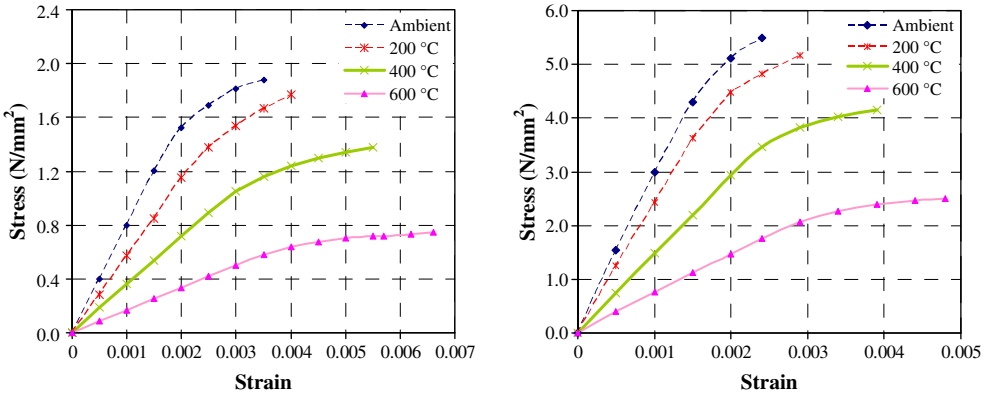

Fig. 8. Average stress–strain relationships for foamed concrete of 650 kg/m^3 (left) and 1000 kg/m^3 (right) at different temperatures.

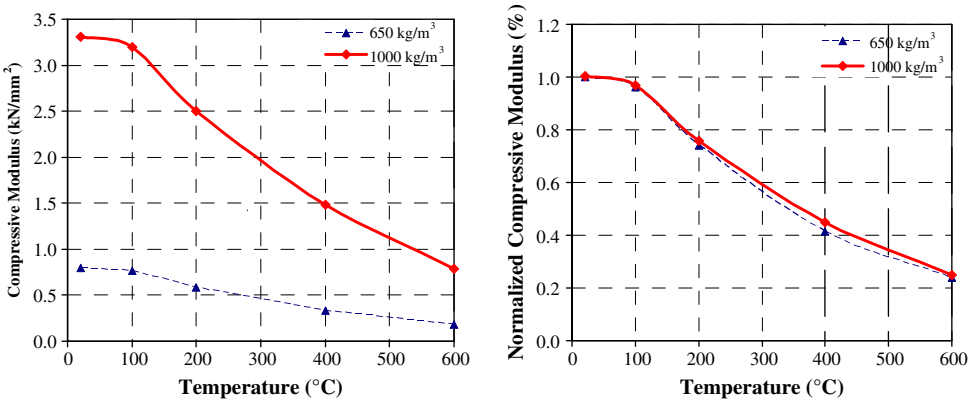

Fig. 9. Compressive modulus (left) and normalized compressive modulus (right) of foamed concrete as a function of temperature.

3.6. Effects of high temperature on foamed concrete failure mode in compression

All the tested foamed concrete specimens exhibited brittle failure at all temperatures levels, failing soon after reaching their peak strength. For the foamed concrete of 650 kg/m^3 density, the end portion of the failed specimens resembled 'double cone pattern' (Fig. 10b) at the top and bottom at 400 °C and when exposed to temperature of 600 °C, the specimens failed in an irregular pattern as shown in Fig. 10c. For foamed concrete of 1000 kg/m^3 density, vertical cracks appeared in the broken specimens with double cone pattern at top and bottom at 400 °C (Fig. 11b); at 600 °C, it experienced the same mode of failure as the foamed concrete of 650 kg/m^3 density (Fig. 11c).

3.7. Effects of high temperature on flexural tensile strength of foamed concrete

Since foamed concrete is a brittle material, the bending test was intended to give a measure of the flexural tensile strength of the foamed concrete. Fig. 12 presents the variation in flexural tensile strength of foamed concrete as a function of temperature. The

(a) at ambient *(b) at 400 °C* *(c) at 600 °C*

Fig. 10. Failure modes of foamed concrete of 650 kg/m^3 density at different temperatures.

(a) at ambient *(b) at 400 °C* *(c) at 600 °C*

Fig. 11. Failure modes of foamed concrete of 1000 kg/m^3 density at different temperatures.

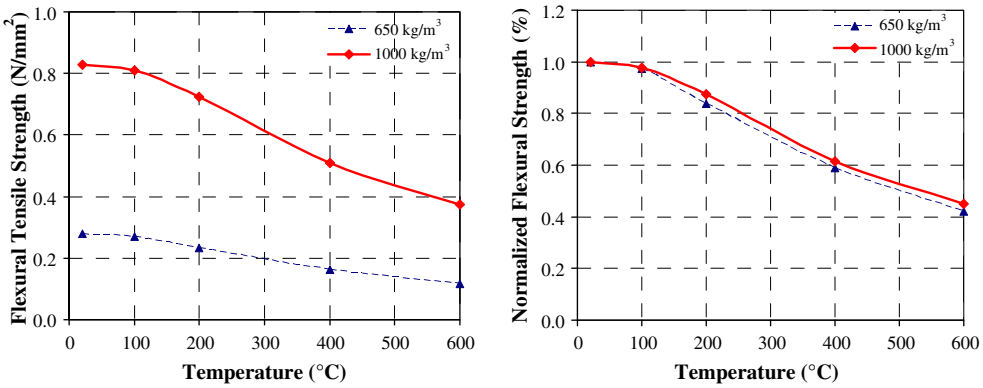

Fig. 12. Flexural tensile strength (left) and normalized flexural tensile strength (right) of foamed concrete as a function of temperature.

reduction in flexural tensile strength of foamed concrete occurred predominantly after 90 °C, regardless of the density of foamed concrete. Consistent with changes in the aforementioned other mechanical properties of foamed concrete, which indicates that the primary mechanism causing degradation is micro cracking, which occurs as the free water and chemically bound water evaporates from the porous body. When the chemical constitution of foamed concrete started to break down between 200 °C and 300 °C due to decomposition of the C-S-H and sulfoaluminate phases ($3CaO{\cdot}Al_2O_3{\cdot}CaSO_4{\cdot}12H_2O$ and $3CaO{\cdot}Al_2O_3{\cdot}3CaSO_4{\cdot}31H$), cracks formed and there was a significant drop in tensile strength. At 400 °C, the tensile strength was about 60% of the initial value for both densities. At 600 °C, the flexural tensile strength achieved was only about 40% and 45% for 650 kg/m^3 and 1000 kg/m^3 densities respectively.

3.8. Effects of temperature on flexural tensile modulus of foamed concrete

Fig. 13 illustrates the changes in flexural modulus of foamed concrete as a function of temperature and compares the flexural modulus with the compressive modulus obtained from the cylinder tests. Although there are some differences, the compressive modulus and flexural modulus values are very similar for both densities and at different temperatures.

3.9. Additional mechanical properties test results

As mentioned earlier, this research also aims to assess and propose mechanical properties prediction equations of foamed concrete based on comparison of the experimental results with

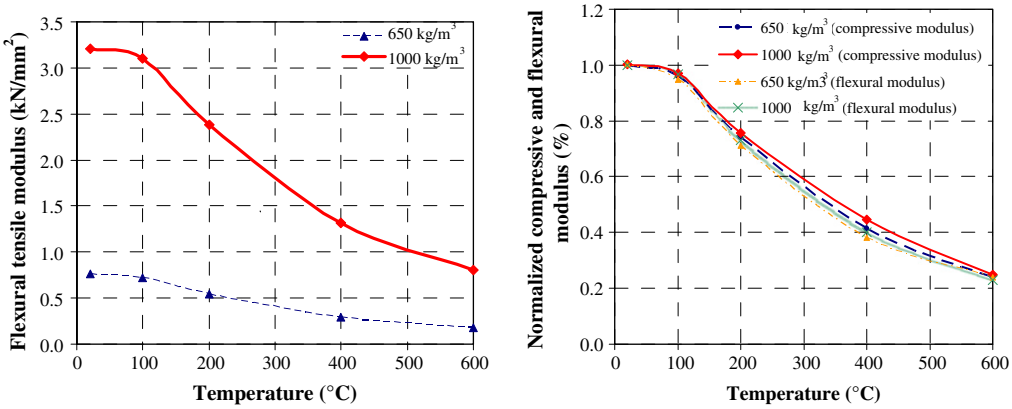

Fig. 13. Flexural tensile modulus (left) and comparison of normalized compressive modulus and flexural tensile modulus (right) of foamed concrete as a function of temperature.

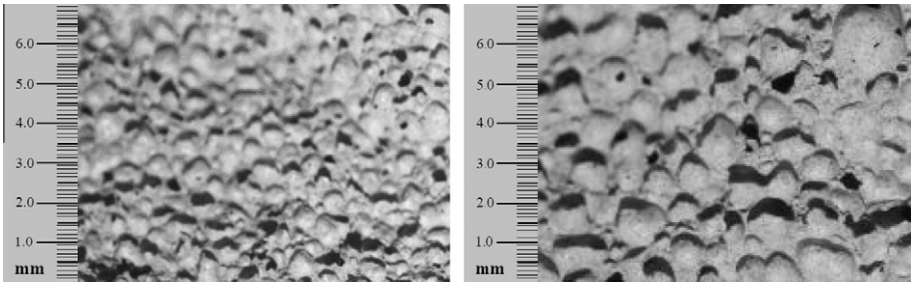

Fig. 14. Void sizes for 1000 kg/m^3 (left) and 650 kg/m^3 (right) densities.

Table 6
Compressive strength and porosity of foamed concrete for 800 kg/m^3, 1200 kg/m^3 and 1400 kg/m^3 density at different temperatures.

Density (kg/m^3)	Average compressive strength (N/mm^2)				Average porosity (%)
	Ambient	200 °C	400 °C	600 °C	
800	3.2	2.9	2.5	1.5	62
1200	11.6	10.4	8.2	4.8	44
1400	15.3	14.0	10.9	6.6	38

Table 7
Modulus of elasticity in compressive of foamed concrete for 800 kg/m^3, 1200 kg/m^3 and 1400 kg/m^3 density at ambient temperature.

Density (kg/m^3)	Average modulus of elasticity in compression (kN/mm^2)			
	Ambient	200 °C	400 °C	600 °C
800	1.8	1.4	0.8	0.5
1200	7.7	5.8	3.5	1.9
1400	10.1	7.6	4.7	2.6

existing models for normal strength concrete. Therefore, to get a good strength–porosity relationship and to observe the influence of voids on the mechanical properties of foamed concrete of this study, additional compression tests were carried out on three additional foamed concrete densities of 800, 1200 and 1400 kg/m^3.

The pore size of foamed concrete was also determined through image analysis tool and Fig. 14 shows an example of images of the internal structure of the 1000 kg/m^3 and 650 kg/m^3 density foamed concrete at ambient temperature. Clearly the void sizes are not uniform. However, these two images clearly indicate that the average void size is principally a function of the foamed concrete density. The average void size tends to increase as the foamed concrete density reduces due to the higher quantity of foam used. From an analysis of the internal images of the two densities of foamed concrete, the average void size of the 650 kg/m^3 and 1000 kg/m^3 density foamed concrete has been determined as 0.72 mm and 0.55 mm respectively. The same analysis of the images were also done for both densities after being exposed to high temperatures and the results indicate that the void size did not change much from that at ambient temperature.

The average foamed concrete compressive strength and porosity values on the three additional foamed concrete densities were specified in Tables 6 and 7 indicated the average modulus of elasticity in compression for all the three densities at different temperatures. The results obtained will be further discussed in Sections 4.1 and 4.2 of this paper.

4. Models for foamed concrete mechanical properties

Since the foamed concrete employed in this study used the same Portland Cement CEM1 as in normal weight concrete for which a number of mechanical property models have been developed, this chapter is intended to assess whether any of these models would be suitable for foamed concrete. A two-stage comparison will be made: assessment of models at ambient temperature and assessment of models for elevated temperatures, based on ambient temperature results.

The intention of this investigation is to propose a procedure to predict the mechanical properties of foamed concrete, based on existing mechanical property predictive models. This procedure is expected to assist manufacturers and future researchers to develop improved products with reduced cost of experimentation. Whilst full-scale tests to regulatory standards will still be necessary for final accreditation purpose, much of this may be avoided by developing a method to predict the mechanical properties of foamed concrete at ambient and elevated temperatures during the development stage.

4.1. Prediction of mechanical properties of foamed concrete at ambient temperature

For foamed concrete at ambient temperature, porosity represents the most important factor in affecting its strength. Therefore it is important to envisage this property correctly in order to obtain a good prediction of overall mechanical properties.

4.1.1. Strength–porosity relationship

Balshin [14] well known strength–porosity relationship will be considered to assess the effects of porosity on compressive strength of foamed concrete, which may be expressed using the following form:

$$f_c = f_{c,0}(1-\varepsilon)^n \tag{4}$$

where f_c is the compressive strength of foamed concrete with porosity ε, $f_{c,0}$ is the compressive strength at zero porosity and n is a coefficient to be determined.

Fig. 15 plots the recorded foamed concrete compressive strength–porosity relationship for different foamed concrete densities at ambient temperature (results of compressive strength presented in Table 6). Using Balshin's strength–porosity relationship, the best correlation is obtained with $n = 2.4$, which was represented by the solid curve in Fig. 15. A correlation coefficient of 0.914 indicates a good correlation between this model and the test results. Thus, the compressive strength of foamed concrete at ambient temperature can be expressed as a power function of porosity as follow:

$$f_c = 39.2(1-\varepsilon)^{2.4} \tag{5}$$

For interest, a similar study was carried out by others for foamed concrete of different densities at ambient temperature. From the experimental results of this study for foamed concrete at different temperatures, the same exercise was undertaken. The results are summarised in Table 8 and compared with results by others for other types of concrete. The n values of foamed concrete obtained in this study show some consistency, but are different from other researchers. The n values of this study are much lower than from other studies, indicating that the foamed concrete of this study suffered less void induced loss of strength.

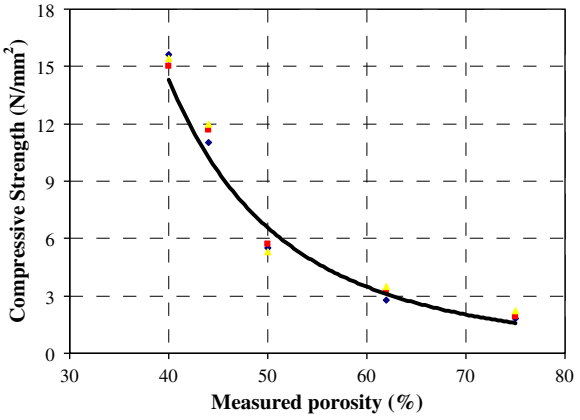

Fig. 15. Compressive strength–porosity relation for foamed concrete at ambient temperature.

Table 8
Comparison of n-values in strength–porosity model for different concretes.

Researchers	Concrete type	Mix composition	Constants	
			$f_{c,0}$ (N/mm^2)	n
Hoff [15]	Foamed concrete	Cement paste	115–290	2.7–3.0
Narayanan and Ramamurthy [16]	Aerated concrete (non autoclaved)	Cement–sand	26.6	3.2
Kearsley and Wainwright [17]	Foamed concrete	Cement with and without fly ash	188	3.1
Present work	Foamed concrete (ambient)	Cement–sand	39.2	2.4
	Foamed concrete (200 °C)		38.5	2.4
	Foamed concrete (400 °C)		28.1	2.4
	Foamed concrete (600 °C)		19.5	2.6

4.1.2. Modulus of elasticity–porosity relationship

As acknowledged by the author, the strength–porosity relationship proposed by Balshin (Eq. (4)) has so far only been used to determine the compressive strength of porous material. This section will explore whether this equation (Eq. (4)) is also appropriate to establish the modulus of elasticity-porosity relationship for foamed concrete. In order to do so, the experimental results of modulus of elasticity for all densities will be plotted as a function of porosity.

Fig. 16 shows the recorded foamed concrete modulus of elasticity-porosity relationship for different foamed concrete densities at ambient temperature (results of modulus of elasticity in Table 7). Surprisingly, the same relationship can be used. The best correlation was found by using $n = 2.8$, shown by the solid curve in Fig. 16. A correlation coefficient of 0.936 indicates strong relationship between the model and the test results. Thus, the following modulus of elasticity–porosity relationship of foamed concrete at ambient temperature is obtained:

$$E_c = 32.9(1-\varepsilon)^{2.8} \tag{6}$$

where E_c is the compressive modulus of foamed concrete at ambient temperature and ε is porosity.

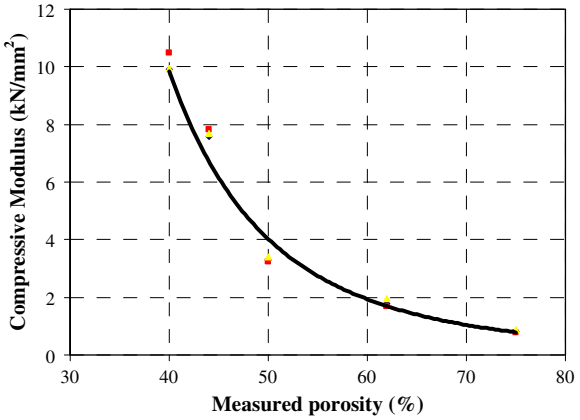

Fig. 16. Modulus of elasticity–porosity relation for foamed concrete at ambient temperature.

Table 9
Summary of $E_{c,0}$ and n values for modulus of elasticity–porosity relationship at different temperatures according to Balshin's model.

Temperature (°C)	Constants	
	$E_{c,0}$ (kN/mm^2)	n
Ambient	32.9	2.8
200	24.7	2.8
400	15.0	2.8
600	8.2	2.8

From the experimental results of this study for foamed concrete at different temperatures, the same exercise was undertaken to obtain the modulus of elasticity–porosity relationships. The results were summarised in Table 9 which shows a constant n value at different temperatures.

4.1.3. Porosity–density relationship

Through using Eqs. (5) and (6), it was possible to obtain an accurate assessment of the compressive strength and modulus of elasticity of foamed concrete. Nevertheless, these models require input of the porosity value. Unfortunately, porosity was a property not frequently measured outside the laboratory, and therefore it is necessary to provide a model to obtain the porosity. The simplest method to calculate the porosity value was to relate it to foamed concrete density. Since the pores inside foamed concrete were created due to addition of foams, by knowing the solid density of cement paste (without foam), one can easily predict the porosity of foamed concrete of any other density using the following equation:

$$\varepsilon = \frac{\rho_{sc} - \rho_{dry}}{\rho_{sc}} \tag{7}$$

where ε is the porosity, ρ_{sc} is the solid density of cement paste (without foam) and ρ_{dry} is the dry density of foamed concrete.

The accuracy of Eq. (7) was checked by comparing the porosity values calculated using Eq. (7) and the measured porosity values using the Vacuum Saturation Apparatus [8] for different foamed concrete densities, like showed in Fig. 17. It should be noted that an average solid density of cement paste (ρ_{sc}) of 2100 kg/m^3 was established through experiment. The agreement is excellent.

4.2. Prediction of mechanical properties of foamed concrete at elevated temperature

A number of concrete mechanical property predictive models have been proposed by others for normal strength concrete. This

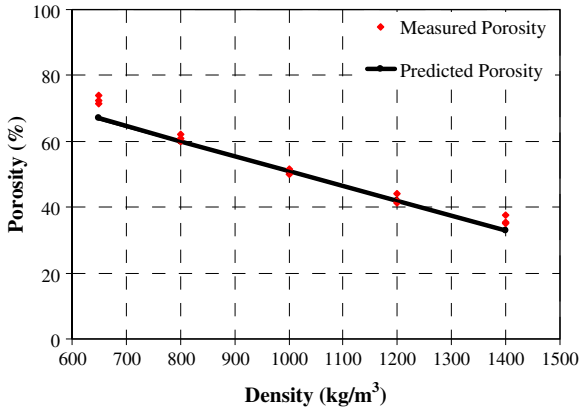

Fig. 17. Comparison of predicted porosity with measured porosity as a function of density.

section was intended to assess the applicability of these models to foamed concrete. In particular, since the Eurocode 2 [18] models are well established, there were the principal models to be considered for adoption unless they gave grossly inaccurate results.

4.2.1. Compressive strength models for concrete at elevated temperatures

Several models have been proposed to estimate concrete compressive strength at high temperatures.

Li and Purkiss [19] presented a review of the available models for the mechanical behavior of concrete at elevated temperatures and provided comparisons between the existing models. Li and Purkiss [19] suggested the following model to predict the compressive strength of concrete at elevated temperatures:

$$f_{cT} = f_c \cdot \left[0.00165 \cdot \left(\frac{T}{100}\right)^3 - 0.03 \cdot \left(\frac{T}{100}\right)^2 + 0.025 \cdot \left(\frac{T}{100}\right) + 1.002\right] \quad (8)$$

where f_{cT} is the concrete compressive strength at elevated temperature, f_c is the concrete compressive strength at ambient temperature and T is temperature in °C.

The Eurocode 2 [18] model is given below:

$$F_{cT} = f_c \quad T \leqslant 100\ ^\circ\mathrm{C} \quad (9a)$$

$$F_{cT} = f_c \cdot (1.067 - 0.00067 \cdot T) \quad 100\ ^\circ\mathrm{C} \leqslant T \leqslant 400\ ^\circ\mathrm{C} \quad (9b)$$

$$F_{cT} = f_c \cdot (1.44 - 0.0016 \cdot T) \quad T \geqslant 400\ ^\circ\mathrm{C} \quad (9c)$$

Hertz [2] in his study on concrete strength for fire safety design had derived an idealised data for the compressive strength of a number of concretes which included test series from more than 400 test comprising approximately 3000 specimens. The data covered a range of concretes with aggregates such as siliceous materials, limestone, granite, sea gravel, pumice, and expanded clay. He then proposed a model for compressive strength of concrete at elevated temperatures that allowed for different types of aggregate to be differentiated as follows:

$$f_{cT} = f_c \cdot \left[\frac{1}{1 + \frac{T}{T_1} + \left(\frac{T}{T_2}\right)^2 + \left(\frac{T}{T_8}\right)^8 + \left(\frac{T}{T_{64}}\right)^{64}}\right] \quad (10)$$

Assuming foamed concrete as a type of lightweight aggregate concrete for application of Hertz's model, then $T_1 = 100{,}000$, $T_2 = 1100$, $T_8 = 800$ and $T_{64} = 940$.

All the above-mentioned predictive models have been assessed and compared with the experimental results for all densities (650, 800, 1000, 1200 and 1400 kg/m^3). Fig. 18 presents a typical comparison of predictions of the models at different temperatures against the experimental results from this study for 650 and 1000 kg/m^3 density. As expected, the results showed that the Hertz [2] model gave much higher results than the test results and was not appropriate for foamed concrete. Both the Eurocode 2 [18] and Li and Purkiss [19] models seem to give good results and suitable for foamed concrete, with the Eurocode 2 predictions being slightly higher than the measured values.

4.2.2. Models for modulus of elasticity of concrete at elevated temperatures

The elastic modulus of concrete would be affected primarily by the same factors influencing its compressive strength [26]. Due to different definitions of modulus of elasticity and the difficulty of precisely calculating this value, it was not surprising that previous researchers have revealed great disparity in the experimental results. In this research, the modulus of elasticity was calculated as the secant modulus corresponding to 0.75 ultimate stress. The following models were considered.

Lu [20] in his study on fire response of reinforced concrete beams, performed an unstressed test procedure to establish the modulus of elasticity of concrete when exposed to high temperatures. He proposed the following tri-linear expression between E_{cT} and T:

$$E_{cT} = (1 - 0.0015 \cdot T) \cdot E_c \quad 20\ ^\circ\mathrm{C} \leqslant T \leqslant 200\ ^\circ\mathrm{C} \quad (11a)$$

$$E_{cT} = (0.87 - 0.00084 \cdot T) \cdot E_c \quad 200\ ^\circ\mathrm{C} \leqslant T \leqslant 700\ ^\circ\mathrm{C} \quad (11b)$$

$$E_{cT} = 0.28 \cdot E_c \quad T \geqslant 700\ ^\circ\mathrm{C} \quad (11c)$$

where E_{cT} and E_c are the modulus of elasticity of concrete at elevated and room temperature, respectively.

Li and Guo [21] carried out an experimental investigation on strength and deformation of concrete under high temperature. They proposed a bi-linear model to predict the modulus of elasticity of concrete as given below:

$$E_{cT} = E_c \quad 20\ ^\circ\mathrm{C} \leqslant T \leqslant 60\ ^\circ\mathrm{C} \quad (12a)$$

$$E_{cT} = (0.83 - 0.0011 \cdot T) \cdot E_c \quad 60\ ^\circ\mathrm{C} \leqslant T \leqslant 700\ ^\circ\mathrm{C} \quad (12b)$$

The Eurocode 2 [18] model did not explicitly give variation of modulus as a function of temperature. However, the compressive modulus may be calculated using the following equation:

$$E_{cT} = \frac{1.5 f_{cT}}{\varepsilon_{oT}} \quad (13)$$

where f_{ct} is the peak stress and ε_{oT} is the strain at peak stress.

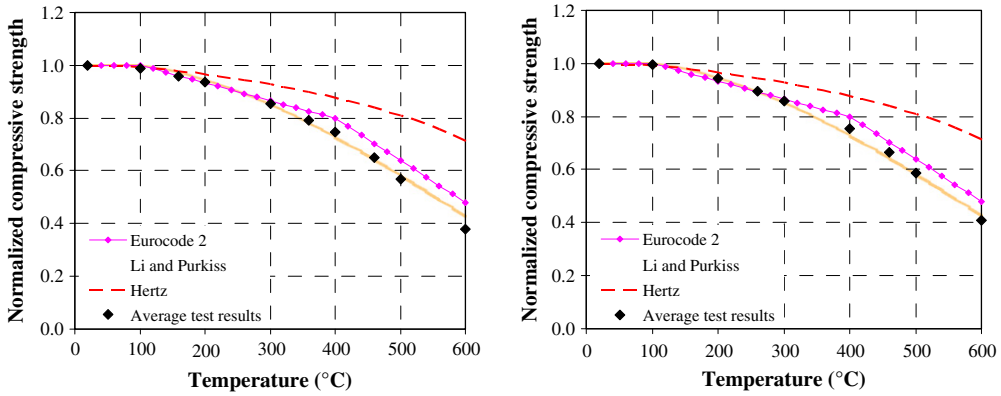

Fig. 18. Comparison of normalized compressive strength–temperature relationships for 650 kg/m^3 (left) and 1000 kg/m^3 (right).

As will be shown later in Section 4.2.3, the strains at peak stress from Eurocode 2 [18] did not agree with the measured values of this research. Therefore, the measured strains will be used in this assessment. This means that this exercise was not predictive, but merely to check whether Eq. (13) is applicable.

Li and Purkiss [19] developed a prediction model for modulus of elasticity of concrete based on published experimental data by Purkiss [27] and the data published in Eurocode 2 [18]. They defined the elastic modulus as the initial tangent modulus and gave the following relationships:

$$E_{cT} = E_c \quad T \leqslant 60^{\circ}\mathrm{C} \tag{14a}$$

$$E_{cT} = \frac{800 - T}{740} \cdot E_c \quad 60\,^{\circ}\mathrm{C} \leqslant T \leqslant 800\,^{\circ}\mathrm{C} \tag{14b}$$

Khennane and Baker [22] in their research on concrete behavior under variable temperature and stress presented a plasticity model using a strain-rate formulation to depict the uniaxial response of concrete when subjected to combined thermal and mechanical actions and they proposed the following equation:

$$E_{cT} = (-0.001282 \cdot T + 1.025641) \cdot E_c \quad 20\,^{\circ}\mathrm{C} \leqslant T \leqslant 800\,^{\circ}\mathrm{C} \tag{15}$$

Fig. 19 compares prediction of the various models with the test results for all densities at different temperatures. Except for the Lu [20] and the Li and Guo [21] models, all the other models give good predictions of the test results, particularly considering the relatively wide scatter of experimental results reported in literature. In conjunction with the conclusion drawn in the last section for compressive strength, both the Eurocode 2 [18] and the Li and Purkiss [19] models may be used. However, as previously mentioned, using the equation of Eurocode 2 [18] was predicated on the assumption that an independent means of obtaining the strains at peak stresses can be established.

4.2.3. Strain at peak compressive stress

For predicting foamed concrete strain at the maximum compressive stress (ε_{oT}), the following models may be considered in regards to the models for cases where concrete specimens were not loaded during the heating process.

(i) Anderberg and Thelandersson [23]

$$\varepsilon_{oT} = (0.00000167 \cdot T) + 0.002666 \quad T \leqslant 800\,^{\circ}\mathrm{C} \tag{16}$$

(ii) Khennane and Baker [22]

$$\varepsilon_{oT} = 0.003 \quad 20\,^{\circ}\mathrm{C} \leqslant T \leqslant 200\,^{\circ}\mathrm{C} \tag{17a}$$

$$\varepsilon_{oT} = (0.00001156 \cdot T) + 0.000686 \quad T \geqslant 200\,^{\circ}\mathrm{C} \tag{17b}$$

(iii) Bazant and Chern [24]

$$\varepsilon_{oT} = (0.0000064 \cdot T) - 0.00216 \quad 20\,^{\circ}\mathrm{C} \leqslant T \leqslant 600\,^{\circ}\mathrm{C} \tag{18}$$

(iv) Li and Purkiss [19]

$$\varepsilon_{oT} = \frac{2 \cdot f_c'}{E_c} + 0.21 \times 10^{-4} \cdot (T - 20) - 0.9 \times 10^{-8} \cdot (T - 20)^2 \tag{19}$$

(v) Eurocode 2 [18]

The Eurocode 2 [18] relationship is reproduced in Table 10.

Table 10
Temperature dependence of the strain at the peak stress point [18].

Temperature (°C)	Strain corresponding to peak stress
0	0.0025
100	0.0040
200	0.0055
300	0.0070
400	0.0100
500	0.0150
600	0.0250
700	0.0250
800	0.0250
900	0.0250
1000	0.0250

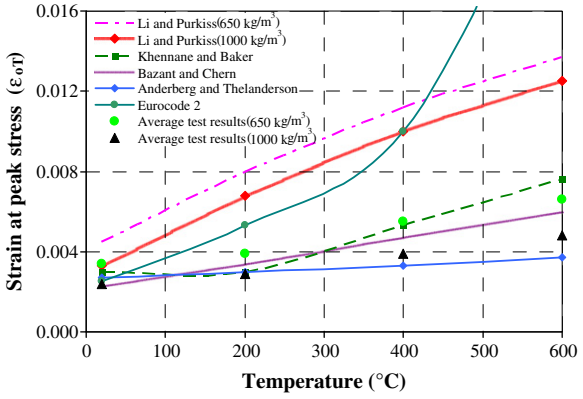

Fig. 20. Comparison of strain at maximum stress–temperature relationships.

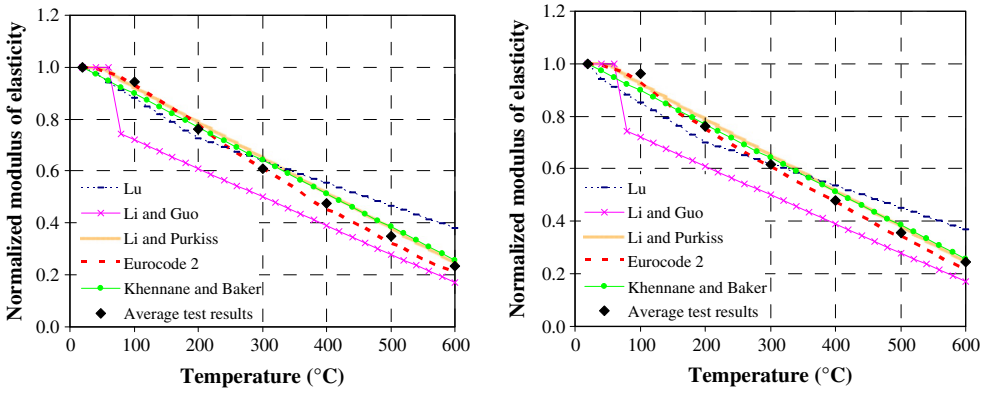

Fig. 19. Comparison of normalized elastic modulus–temperature relationships for 650 kg/m^3 (left) and 1000 kg/m^3 (right).

Fig. 20 provides a comparison of the above-mentioned prediction models with the average test results for the two densities at different temperatures. It is clear from Fig. 20 that the Eurocode 2 [18] model is not suitable. The model of Li and Purkiss [19] provides the upper bound for ε_{oT} and the model of Anderberg and Thelandersson [23] provided the lower bound. The results of the three remaining models gave close agreement with the experimental results. Out of all the models, the Bazant and Chern [24] prediction appears to give the best agreement with these experimental results.

Although the Eurocode 2 [18] values of strain at peak stress cannot be used for foamed concrete, the Eurocode 2 equation (Eq. (13)) does reveal that the strain at peak stress is simply 1.5 times the elastic strain at peak stress. In fact, based on the experimental results of this research, the strain at peak stress is about 1.78 times the elastic strain at peak stress.

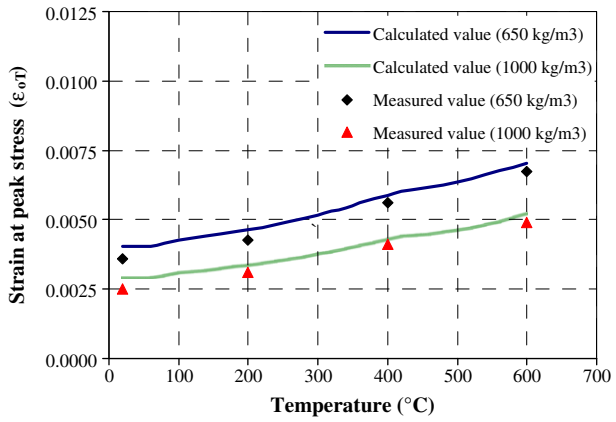

Fig. 21. Comparison of calculated and measured strain at peak stress values for 650 and 1000 kg/m^3 densities at different temperatures.

For analysis of structural behavior of foamed concrete, it is more important to correctly predict the modulus of elasticity than the strain at peak stress. Therefore, this research recommends using the Li and Purkiss equation (Eq. (14)) to directly predict the modulus of elasticity change as a function of temperature. The strain at peak stress can then be obtained by the following two steps: (i) using the Eurocode 2 model (Eq. (9)) to predict the foamed concrete strength at different temperatures; (ii) multiplying the elastic strain at peak stress by a constant ratio of 1.78 as obtained from this research. Fig. 21 compares values of the calculated and measured strain at peak stress for both densities at different temperatures. The agreement is excellent.

4.2.4. Stress–strain relationship of concrete exposed to elevated temperatures

The three models which will be considered for the stress–strain relationship of foamed concrete were the Anderberg and Thelandersson [23] model, Lie and Lin [25] model and the Eurocode 2 [18] model.

(i) Anderberg and Thelandersson model [23]

This model was based on transient tests and the ascending compressive part of the relationship is:

$$f'_{cT} = E_{cT} \cdot \left[\varepsilon_{cT} - \frac{\varepsilon_{cT}^2}{2 \cdot \varepsilon_{oT}}\right] \tag{20}$$

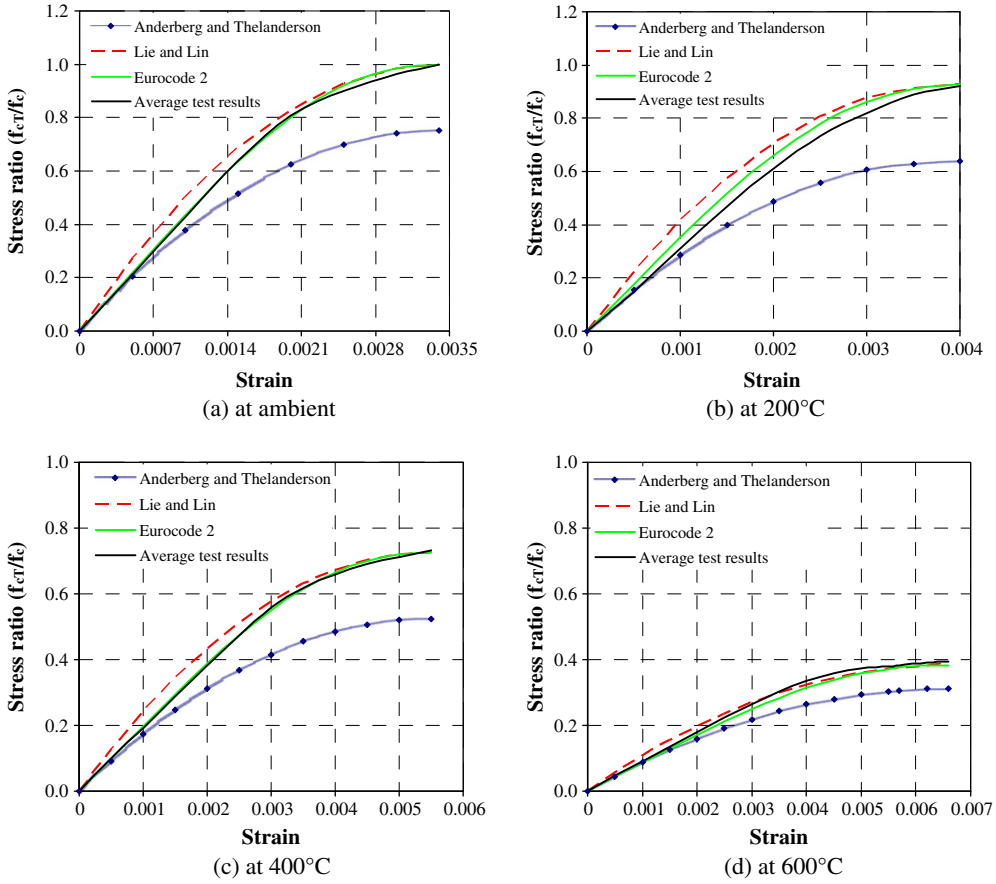

Fig. 22. Stress–strain curves for 650 kg/m^3 density at different temperatures.

where E_{cT} is the modulus of elasticity of concrete at elevated temperature.

(ii) Lie and Lin model [25]

This model includes an ascending and a descending branch. However, since only the ascending branch of foamed concrete stress–strain relationship could be obtained, only the ascending branch equation will be given, which was as follows.

$$f'_{cT} = f_{cT} \cdot \left[1 - \left(\frac{\varepsilon_{oT} - \varepsilon_{cT}}{\varepsilon_{oT}}\right)^2\right] \quad \varepsilon_{cT} \leqslant \varepsilon_{oT} \tag{21}$$

where f'_{cT} is the concrete compressive stress at elevated temperature, f_{cT} is the concrete compressive strength at elevated temperature, ε_{cT} is the concrete strain at elevated temperature and ε_{oT} is the strain at the maximum concrete stress.

(iii) Eurocode 2 model [18]

The Eurocode 2 equation is:

$$f'_{cT} = \frac{3\varepsilon_{cT} f_{cT}}{\varepsilon_{oT}\left(2 + \left(\frac{\varepsilon_{cT}}{\varepsilon_{oT}}\right)^3\right)} \tag{22}$$

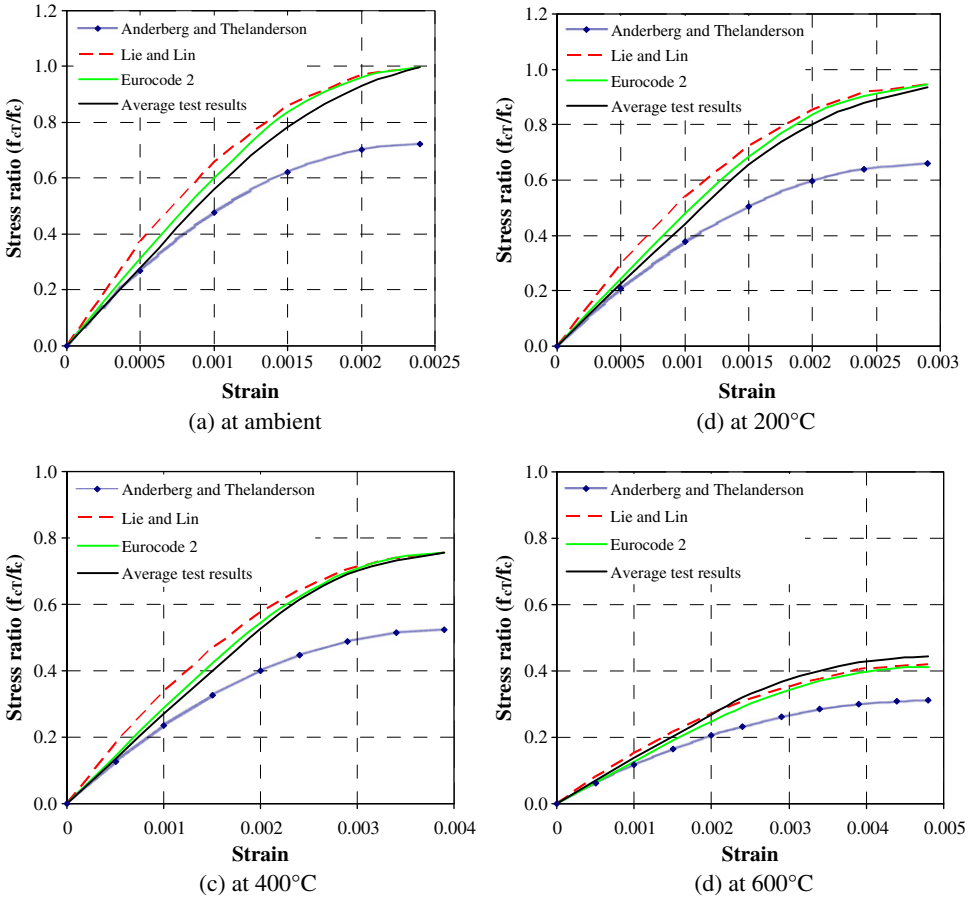

Fig. 23. Stress–strain curves for 1000 kg/m^3 density at different temperatures.

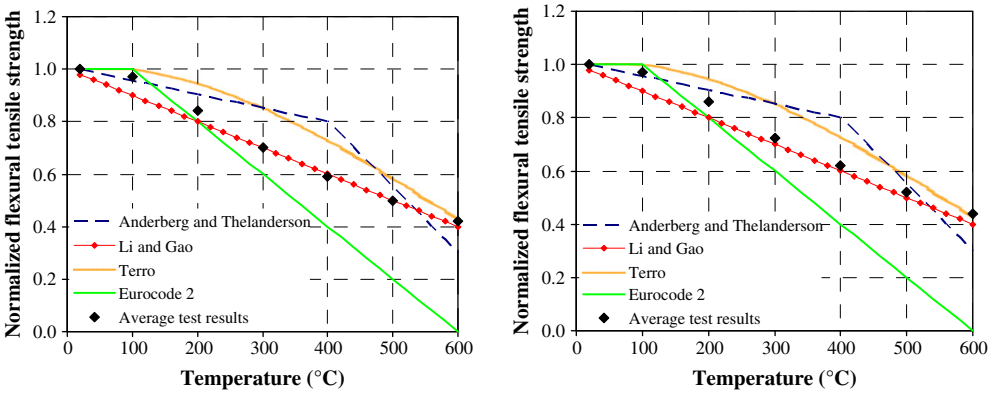

Fig. 24. Comparison of flexural tensile strength–temperature relationships for 650 kg/m^3 (left) and 1000 kg/m^3 (right).

All three models require input of the foamed concrete peak stress (f_{cT}) and strain at peak stress (ε_{cT}). For this exercise, the measured values were used so that this comparison does suffer from any inaccuracy in prediction of these input values.

Figs. 22a–d and 23a–d compare predictions of the different models with the average test results for the two densities at different temperatures (ambient, 200 °C, 400 °C and 600 °C). Except for the Anderberg and Thelandersson [23] model, Lie and Lin [25] and Eurocode 2 [18] model were almost identical and in good agreement with the experimental results for all densities at different temperatures. Since the Eurocode 2 [18] model is well established and accepted for use in fire engineering design of concrete structures, the author suggests adopting the Eurocode 2 [18] model.

4.2.5. Flexural tensile strength of concrete exposed to elevated temperatures

There was very limited research related to tensile strength of concrete at elevated temperatures. Nevertheless, a few researchers such as Anderberg and Thelandersson [23], Li and Guo [21] and Terro [28] have proposed prediction equations.

The Anderberg and Thelandersson [23] model was:

$$f_{crT} = f_{cr} \cdot (-0.000526 \cdot T + 1.01052) \quad 20\,^{\circ}\mathrm{C} \leqslant T \leqslant 400\,^{\circ}\mathrm{C} \tag{23a}$$

$$f_{crT} = f_{cr} \cdot (-0.0025 \cdot T + 1.8) \quad 400\,^{\circ}\mathrm{C} \leqslant T \leqslant 600\,^{\circ}\mathrm{C} \tag{23b}$$

$$f_{crT} = f_{cr} \cdot (-0.0005 \cdot T + 0.6) \quad 600\,^{\circ}\mathrm{C} \leqslant T \leqslant 1000\,^{\circ}\mathrm{C} \tag{23c}$$

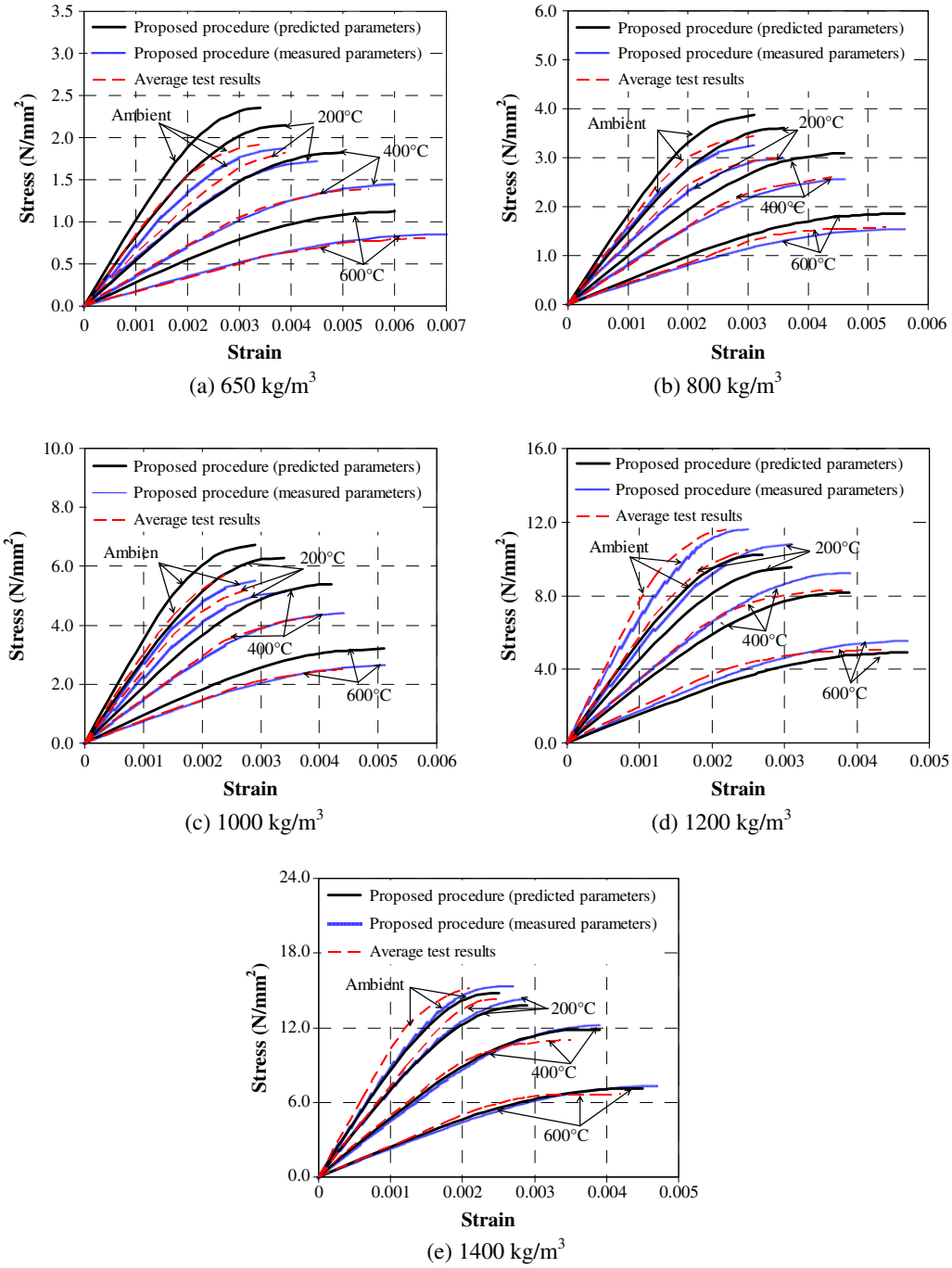

Fig. 25. Comparison between the predicted stress–strain relationships using the proposed procedure and the average experimental results for both densities.

where f_{crT} and f_{cr} are the tensile strength of concrete at elevated temperature and ambient temperature respectively and T is temperature in °C.

Li and Guo [21] suggested the following equation based on the experimental results for tensile strength of concrete under high temperatures:

$$f_{crT} = f_{cr} \cdot (1 - 0.001 \cdot T) \quad 20\,^{\circ}\mathrm{C} \leqslant T \leqslant 1000\,^{\circ}\mathrm{C} \tag{24}$$

Terro [28] performed a numerical modeling of the behavior of concrete structures under fire condition and make recommendation as follows:

$$f_{crT} = f_{cr} \cdot \frac{f_{cT}}{f_c} \tag{25}$$

where f_{cT} is the concrete compressive strength at elevated temperature, f_c is the concrete compressive strength at ambient temperature.

Eurocode 2 [18] gives:

$$f_{crT} = f_{cr} \quad 20\,^{\circ}\mathrm{C} \leqslant T \leqslant 100\,^{\circ}\mathrm{C} \tag{26a}$$

$$f_{crT} = f_{cr} \cdot (-0.002 \cdot T + 1.2) \quad 100\,^{\circ}\mathrm{C} \leqslant T \leqslant 600\,^{\circ}\mathrm{C} \tag{26b}$$

Fig. 24 compares the prediction of the aforementioned models for foamed concrete density of 650 kg/m^3 and 1000 kg/m^3 at different temperatures against the experimental results from this study. It is clear that the model of Anderberg and Thelandersson [23] and Terro [28] provide the upper bound for f_{ctT}, while the model of Li and Gao [21] provides the lower bound for both densities. The Eurocode 2 [18] model did not seem to fit well with the experimental results. Overall, the model proposed by Li and Gao [21] seemed to provide the best agreement with the experimental results.

4.2.6. Summary of combined predictive models

The mechanical properties of foamed concrete that influence the stress–strain relationship were the foamed concrete strength, initial modulus of elasticity and strain at maximum stress. They experience significant changes at elevated temperatures. The foamed concrete strength and initial modulus of elasticity decrease, while the absolute value of the strain at peak stress increases.

After a comprehensive assessment of all existing mechanical property predictive models, the following procedure may be used to predict the mechanical properties of foamed concrete at high temperatures:

1. Obtaining dry density (ρ_{dry}) of foamed concrete.
2. Obtaining the solid density of cement paste (without foam) and then calculate the porosity (ε) of foamed concrete using Eq. (7).
3. Calculating the ambient temperature compressive strength (f_c) and modulus of elasticity (E_c) of foamed concrete using Eqs. (5) and (6) respectively. Values of 39.2 N/mm^2 and $n = 2.4$ for the compressive strength and 32.9 N/mm^2 and $n = 2.8$ for the compressive modulus of elasticity should be used.
4. Eurocode 2 model (Eq. (9)) to calculate foamed concrete compressive strength (f_{cT}) at high temperatures was used.
5. Calculating foamed concrete modulus of elasticity (E_{cT}) at high temperatures using the Li and Purkiss model (Eq. (14)).
6. Multiplying the elastic strain at peak stress by 1.78 to give the strain at peak stress.
7. Using the Eurocode 2 equation (Eq. (22)) to calculate and plot the stress–strain relationship of foamed concrete.
8. Calculating the tensile strength of foamed concrete using the equation (Eq. (24)) of Li and Guo [21].

4.3. Proposed procedure using combined predictive models

The procedure presented in Section 4.2.6 has been implemented for all the tests carried out in this study. This section presents detailed comparison between the predicted stress–strain relationships using the above procedure and the experimental results. Fig. 25a–e showed the comparison between the predicted stress–strain relationships using the proposed procedure and the average experimental results of different densities (650, 800, 1000, 1200 and 1400 kg/m^3) at different temperatures. Shown in these figures were also predicted stress–strain relationships if the measured ambient temperature strength and modulus of elasticity values were used instead of using the proposed strength–porosity (Eq. (5)) and modulus of elasticity–porosity (Eq. (6)) relationships. Overall the agreement was good, demonstrating the feasibility of using the proposed procedure to predict the mechanical properties of foamed concrete of different densities at different temperatures by only knowing one single value of dry density (ρ_{dry}) of foamed concrete. However, there was some inaccuracy in the stress–strain relationships using the proposed procedure which was primarily a result of some inaccuracy in the proposed strength–porosity and modulus of elasticity–porosity relationships at ambient temperature. These figures showed that if the measured strength and modulus of elasticity were used, the predicted stress–strain relationships were in very close agreement with the test results. Therefore, it was recommended that ambient temperature mechanical tests should still be carried out to obtain the strength and modulus of elasticity values, rather than relying on the strength–porosity and modulus of elasticity–porosity models. The other high temperature mechanical property models (compressive strength ratio–temperature relationship, modulus of elasticity ratio–temperature relationship, strain at peak stress and stress–strain relationship) gave very accurate results.

5. Conclusions

This paper has presented the results of a comprehensive study to quantify the mechanical properties of foamed concrete at elevated temperatures. Compressive cylinder tests and three point bending tests were carried out for a range of foamed concrete densities at different temperatures to 600 °C. The mechanical properties included compressive cylinder strength, compressive modulus of elasticity, compressive stress–strain relationship, strain at the maximum compressive stress, porosity, flexural bending strength and modulus of elasticity. The experimental results were then compared with predictive models based on normal strength concrete. From the experimental and comparative results, the following conclusions may be drawn:

1. The experimental results consistently demonstrated that the loss in stiffness for cement based material like foamed concrete at elevated temperatures occurs predominantly after about 90 °C, regardless of density. This indicates that the primary mechanism causing stiffness degradation is microcracking, which occurs as water expands and evaporates from the porous body.
2. Reducing the density of foamed concrete reduces its strength and stiffness. However, for foamed concrete of different densities, the normalized strength and stiffness (ratio of elevated temperature value to ambient temperature value) – temperature relationships are very similar.
3. The porosity of foamed concrete is principally a function of density and changes little at different temperatures. Thus, the change in mechanical property of foamed concrete at high tem-

peratures comes principally from changed chemical components of foamed concrete.

4. Given that the mechanical properties of foamed concrete come from Portland Cement CEM1, it has been confirmed that the reduction in mechanical properties of foamed concrete can be predicted using the mechanical property models for normal strength concrete. The Balshin equation (Eq. (4)) may be used to calculate both the ambient temperature compressive strength and compressive modulus of elasticity, as a function of porosity of foamed concrete. Nevertheless, for improved accuracy, ambient temperature mechanical property tests are still recommended.
5. For compressive strength at elevated temperatures, the well accepted Eurocode 2 [18] model is applicable and Li and Purkiss [19] model may be used to predict the compressive modulus of elasticity at elevated temperatures. For foamed concrete, the total strain at peak stress is approximately 1.78 times the elastic strain at peak stress. The Eurocode 2 [18] equation may be used to obtain the compressive stress–strain relationship of foamed concrete.
6. The model of Li and Gao [21] gave good prediction of the flexural tensile strength of foamed concrete at elevated temperatures.

Acknowledgements

The first author gratefully acknowledges financial support for this research provided by Universiti Sains Malaysia under USM Incentive Grant (Ref. No. 2011/0348).

References

[1] Khoury GA, Majorana CE, Pesavento F, Schrefler BA. Modelling of heated concrete. Mag Concr Res 2002;54:77–101.
[2] Hertz KD. Concrete strength for fire safety design. Mag Concr Res 2005;57:445–53.
[3] Ai H, Young JF, Scherer GW. Thermal expansion kinetics: method to measure permeability of cementitious materials: II. Application to hardened cement pastes. J Am Ceram Soc 2001;84:385–91.
[4] BS EN 197-1. Cement: composition, specifications and conformity criteria for low heat common cements. London: British Standards Institution; 2000.
[5] BS EN 12620. Aggregates for concrete. London: British Standards Institution; 2002.
[6] Md Azree OM. Effect of using additives to the compressive strength of lightweight foamed concrete. Master dissertation, School of Housing, Building and Planning, University of Science Malaysia, Penang; 2004.
[7] Phan LT, Carino NJ. Code provisions for high strength concrete strength temperature relationship at elevated temperatures. J Mater Struct 2003;36:91–8.
[8] Cabrera JG, Lynsdale CJ. A new gas permeameter for measuring the permeability of mortar and concrete. Mag Concr Res 1988;40:177–82.
[9] Taylor HFW. Cement chemistry. London: Academic Press; 1992.
[10] Kalifa P, Tsimbrovska M. Comportement des BHP à hautes températures – Etat de la question et résultats expérimentaux. Cahier du CSTB, n°3078; 1998.
[11] Gallé C, Sercombe J. Permeability and pore structure evolution of silico-calcareous and hematite high-strength concretes submitted to high temperatures. J Mater Struct 2001;34:619–28.
[12] Ye G, Liu X, De Schutter G, Taerwe L, Vandevelde P. Phase distribution and microstructural changes of SCC at elevated temperatures. J Cem Concr Res 2007;37:978–87.
[13] Khoury GA. Compressive strength of concrete at high temperatures: a reassessment. Mag Concr Res 1992;44:291–309.
[14] Balshin MY. Dependence of mechanical properties of metal powders on porosity and limiting properties of metal–ceramic materials. Dokl Akad Nauk UzSSR 1949;67:831–4.
[15] Hoff GC. Porosity–strength considerations for cellular concrete. J Cem Concr Res 1972;2:91–100.
[16] Narayanan N, Ramamurthy K. Prediction relations based on gel-pore parameters for the compressive strength of aerated concrete. Concr Sci Eng 2000;1:206–12.
[17] Kearsley EP, Wainwright PJ. The effect of porosity on the strength of foamed concrete. J Cem Concr Res 2002;32:233–9.
[18] CEN 1992-1-2. Eurocode 2. Design of concrete structures. Part 1.2: general rules – structural fire design. European Committee for Standardisation Document: Brussels; 2004.
[19] Li L, Purkiss JA. Stress–strain constitutive equations of concrete material at elevated temperatures. J Fire Saf 2005;40:669–86.
[20] Lu ZhD. A research on fire response of reinforced concrete beams. PhD thesis, Tongji University; 1989.
[21] Li W, Guo ZhH. Experimental investigation on strength and deformation of concrete under high temperature. Chin J Build Struct 1993;14:8–16.
[22] Khennane A, Baker G. Uniaxial model for concrete under variable temperature and stress. J Eng Mech, ASCE 1993;119:1507–25.
[23] Anderberg Y, Thelandersson S. Stress and deformation characteristics of concrete at high temperatures: experimental investigation and material behavior model. Bulletin 54. Lund, Sweden: Lund Institute of Technology; 1976.
[24] Bazant P, Chern JC. Stress-induced thermal and shrinkage strains in concrete. J Eng Mech, ASCE 1987;113:1493–511.
[25] Lie TT, Lin TD. Fire performance of reinforced concrete columns. In: ASTM STP 882, fire safety: science and engineering; 1985, p. 176–205.
[26] Malhotra HL. Design of fire-resisting structures. London: Surrey University Press; 1982.
[27] Purkiss JA. Fire safety engineering – design of structures. Oxford: Butterworth Heinemann; 1996.
[28] Terro MJ. Numerical modeling of the behavior of concrete structures in fire. J Am Concr Inst Struct 1998;95:183–93.